

Dimension of Activity in Random Neural Networks

David G. Clark,^{*} L.F. Abbott,[†] and Ashok Litwin-Kumar[‡]

Center for Theoretical Neuroscience, Columbia University, New York, New York 10027, USA

(Dated: August 9, 2022)

Neural networks are high-dimensional nonlinear dynamical systems that process information through the coordinated activity of many interconnected units. Understanding how biological and machine-learning networks function and learn requires knowledge of the structure of this coordinated activity, information contained in cross-covariances between units. Although dynamical mean field theory (DMFT) has elucidated several features of random neural networks—in particular, that they can generate chaotic activity—existing DMFT approaches do not support the calculation of cross-covariances. We solve this longstanding problem by extending the DMFT approach via a two-site cavity method. This reveals, for the first time, several spatial and temporal features of activity coordination, including the effective dimension, defined as the participation ratio of the spectrum of the covariance matrix. Our results provide a general analytical framework for studying the structure of collective activity in random neural networks and, more broadly, in high-dimensional nonlinear dynamical systems with quenched disorder.

Neural circuits generate cognition, sensation, and behavior through the coordinated activity of many synaptically coupled neurons. Similarly, artificial neural networks solve machine-learning tasks through distributed computations among many neuron-inspired units, with couplings trained via gradient descent. Understanding the collective structure of the activity in such high-dimensional dynamical systems is a central problem in neuroscience and artificial intelligence. This problem is complicated by the nonlinearity of biological and artificial neurons and by the heterogeneity of the couplings.

In addressing this problem, studying networks with random couplings has been fruitful for a variety of reasons [1–4]. First, the dynamics of gradient descent in artificial networks depends sensitively on the initial couplings, which are random [5–8]. Second, random couplings provide a computational substrate for many tasks, the core idea of reservoir computing [9–12]. Third, random couplings are a parsimonious model of background connectivity upon which structure can be introduced [13]. In certain cases, artificial networks trained via gradient descent learn low-rank perturbations on their initial random connectivity [14, 15]. Finally, random networks provide a model of asynchronous cortical dynamics observed *in-vivo* [16]. Outside of neuroscience and machine learning, high-dimensional nonlinear dynamical systems with quenched disorder are important models in physics, ecology, chemistry, and the social sciences [1, 13, 17–28].

Such disordered dynamical systems are commonly studied using dynamical mean-field theory (DMFT), which reduces the high-dimensional dynamics to a self-consistent single-site problem. DMFT has revealed several properties of these systems, including their ability

to generate chaotic dynamics. However, key properties of the emergent structure are not visible within single-unit activities, but only within cross-covariances, which are inaccessible within existing DMFT approaches. One such property is the effective dimension, which measures the degree of coordination of network activity in terms of the approximate number of excited collective modes [29–36]. Recent works have shown that this quantity determines a network’s ability to classify inputs [37–40], learn via Hebbian plasticity [37, 41], generalize learned structure [37, 41, 42], and generate dynamics [12, 43]. If the effective dimension is low, the network dynamics can be inferred from a small number of units [44–47]. Because we have lacked, until now, a theory of cross-covariances in random nonlinear networks, it has been impossible to study these key aspects of network function analytically in networks displaying rich internal dynamics.

In this paper, we surmount this problem by developing a two-site DMFT based on the cavity method, yielding an intuitive mean-field picture of a perturbatively coupled pair of units through which statistics of time-lagged cross-covariances, and thus the effective dimension, are calculated. We develop this theory for the illustrative case of the network model of Sompolinsky *et al.* [1], which displays a generic transition to chaos above a critical coupling variance [20]. Our framework applies more generally to high-dimensional nonlinear dynamical systems with quenched disorder.

Our calculation of the effective dimension reveals that collective activity is predominantly confined to a subspace of extensive, but fractionally low, dimension, providing an analytical signature of extensive chaos as has been suggested by simulations [29, 30, 33]. Our theory additionally reveals that collective modes have a typical timescale much slower than that of individual neurons.

Model & Order Parameters: The network we study has N units with current variables $x_i(t)$ and response variables $\phi_i(t) = \phi(x_i(t))$, where $\phi(\cdot)$ is an odd-symmetric

^{*} dgc2138@cumc.columbia.edu, he/him

[†] lfa2103@columbia.edu

[‡] a.litwin-kumar@columbia.edu

sigmoid-shaped function with $\phi(\pm\infty) = \pm 1$. The system has quenched disorder in its random Gaussian couplings, $J_{ij} \sim \mathcal{N}(0, g^2/N)$. The network dynamics are

$$(1 + \partial_t) x_i(t) = \sum_j J_{ij} \phi_j(t). \quad (1)$$

For large N , the network is quiescent (i.e., the trivial fixed point, $x_i(t) = 0$, is globally stable) for $g < g_{\text{crit}}$ and chaotic for $g > g_{\text{crit}}$, where $g_{\text{crit}} = 1/\phi'(0)$. The classic DMFT of [1] is based on the fact that, to leading order in a large- N expansion, the input currents are zero-mean Gaussian fields with vanishing cross-covariances. Thus, the network decouples into N non-interacting processes,

$$(1 + \partial_t)x(t) = \eta(t), \quad (2)$$

where $\eta(t)$ is an effective Gaussian field. Throughout, we assume a statistically stationary state. The DMFT can be used to compute the autocovariance functions

$$C_a(\tau) = \langle a_i(t)a_i(t+\tau) \rangle_{\mathbf{J}} = \langle a(t)a(t+\tau) \rangle_{\eta}, \quad (3)$$

where we have adopted the notation $a \in \{x, \phi\}$. $C_x(\tau)$ obeys Newtonian dynamics, $\partial_\tau^2 C_x(\tau) = -\partial_{C_x} V(C_x)$, in a Mexican-hat potential $V(C_x)$ [1]. A key parameter in our theory is one plus the curvature of $V(C_x)$ at zero,

$$\nu = 1 + \partial_{C_x}^2 V|_{C_x=0} = g^2 \alpha^2, \quad (4)$$

where $\alpha = \langle \phi'(t) \rangle_{\eta}$. Due to the Mexican-hat shape of the potential, $\nu < 1$. For $\tau \gg 1$, $C_x(\tau) \sim \exp(-\sqrt{1-\nu}\tau)$.

Crucially, cross-covariances are ignored within the DMFT; the network is assumed to fully decouple. In this paper, we go beyond existing DMFT approaches by calculating the structure of cross-covariances, which scale as $\sim 1/\sqrt{N}$. This requires computation of the disorder-averaged variance of the time-averaged cross-covariance. We define the intensive spatiotemporal order parameter

$$\psi_a(\tau, \tau') = N \langle \langle a_i(t)a_j(t+\tau) \rangle_i \langle a_i(t')a_j(t'+\tau') \rangle_{t'} \rangle_{\mathbf{J}}, \quad (5)$$

where $i \neq j$. Since the system is self-averaging, the average over \mathbf{J} is equal to an average over all pairs of distinct units in a single large network. Our main result is that, for $N \rightarrow \infty$, $\psi_a(\tau, \tau')$ is given in Fourier space by

$$\begin{aligned} \hat{\psi}_a(\omega_1, \omega_2) &= \gamma_a \left[1 + \frac{\nu^2}{(1 + \omega_1^2)(1 + \omega_2^2) - \nu^2} \right] \\ &\times \left[1 + 2\text{Re} \left\{ \frac{\nu}{(1 + i\omega_1)(1 + i\omega_2) - \nu} \right\} \hat{\Phi}_a(\omega_1, \omega_2) \right] \\ &\times \hat{C}_x(\omega_1) \hat{C}_x(\omega_2), \end{aligned} \quad (6)$$

where $\gamma_x = 1$, $\gamma_\phi = \alpha^4$, $\hat{\Phi}_x(\omega_1, \omega_2) = 2 - \nu^2 / ((1 + \omega_1^2)(1 + \omega_2^2))$, and $\hat{\Phi}_\phi(\omega_1, \omega_2) = (1 + \omega_1^2)(1 + \omega_2^2) / \nu^2$. As we will show, this quantity encodes important spatiotemporal properties of activity, including the effective dimension and collective timescales. It is remarkable that $\psi_a(\tau, \tau')$

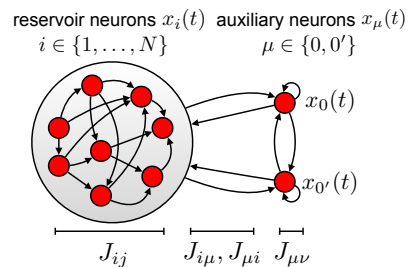


FIG. 1. Overview of the two-site cavity DMFT. A cavity is created at the sites of two auxiliary neurons while the rest of the network, the reservoir, generates chaotic activity. The auxiliary neurons are then introduced; their effect is felt perturbatively by the reservoir. Dynamical equations for the auxiliary neurons yield a pair of perturbatively coupled mean-field equations representing a pair of neurons. Self-consistency conditions are constructed by noting that the auxiliary pair is statistically equivalent to any reservoir pair.

admits a closed-form solution in terms of $C_a(\tau)$, as the latter requires numerical integration of Newtonian dynamics. Note that the dependence of $\psi_a(\tau, \tau')$ on the form of the nonlinearity $\phi(\cdot)$ occurs only through $C_a(\tau)$ and ν . The inequality $\hat{\Phi}_x(\omega_1, \omega_2) \neq \hat{\Phi}_\phi(\omega_1, \omega_2)$ indicates that the x variables possess a non-Gaussian joint distribution (cf. Price's theorem for Gaussian variables [48]).

Two-Site Cavity Dynamical Mean-Field Theory: Our derivation is based on the cavity method [49, 50], a powerful and intuitive technique for the analysis of disordered systems. We use a dynamical version [23, 51] with a two-site cavity [52] (Fig. 1). We add to the network two auxiliary neurons with indices 0 and 0', and refer to the original N neurons as the reservoir. We use Latin and Greek indices for reservoir and auxiliary neurons indices, respectively. The auxiliary neurons are bidirectionally connected to the reservoir through the couplings $J_{i\mu}$ and $J_{\mu i}$, and to one another through the off-diagonals of $J_{\mu\nu}$.

In the absence of the auxiliary neurons, reservoir neurons follow trajectories $x_i(t)$. When the auxiliary neurons are introduced, these trajectories are perturbed by $\delta x_i(t) = \int_{-\infty}^t dt' \sum_j \chi_{ij}(t, t') \sum_\mu J_{j\mu} \phi_\mu(t')$, where $\chi_{ij}(t, t') = \delta x_i(t) / \delta I_j(t')$ is the linear susceptibility with $I_i(t)$ an infinitesimal source term added to the right-hand side of Eq. 1. By causality, $\chi_{ij}(t, t') = 0$ for $t < t'$. Inserting the perturbed trajectories $x_i(t) + \delta x_i(t)$ into Eq. 1 yields dynamical equations for the auxiliary neurons,

$$(1 + \partial_t) x_\mu(t) = \eta_\mu(t) + \frac{1}{\sqrt{N}} \sum_\nu \left(\int_{-\infty}^t dt' \kappa_{\mu\nu}(t, t') \phi_\nu(t') + \mathcal{J}_{\mu\nu} \phi_\nu(t) \right), \quad (7)$$

where we have defined the order-one variables

$$\eta_\mu(t) = \sum_i J_{\mu i} \phi_i(t), \quad (8a)$$

$$\kappa_{\mu\nu}(t, t') = \sqrt{N} \sum_{ij} J_{\mu i} J_{j\nu} \phi'_i(t) \chi_{ij}(t, t'), \quad (8b)$$

$$\mathcal{J}_{\mu\nu} = \sqrt{N} J_{\mu\nu}. \quad (8c)$$

The fields $\eta_\mu(t)$ and $\kappa_{\mu\nu}(t, t')$ are random due to the quenched disorder. Eq. 7 thus becomes a two-dimensional system of perturbatively coupled mean-field equations describing a *pair* of neurons, generalizing Eq. 2 describing a single neuron. The presence of the nonlinearity $\phi(\cdot)$ in the terms coupling $x_0(t)$ and $x_{0'}(t)$ induces a non-Gaussian joint distribution over these variables. Three effects contribute to the cross-covariance between neurons 0 and $0'$ at leading order, $1/\sqrt{N}$. First, neurons 0 and $0'$ receive feedforward input from the reservoir via distinct random projections, resulting in a temporal cross-covariance of order $1/\sqrt{N}$ between $\eta_0(t)$ and $\eta_{0'}(t)$ (in contrast to models in which neurons receive uncorrelated background fluctuations). Second, neuron $0'$ projects to the reservoir, producing reverberating activity that is read out by neuron 0, and vice versa. This is captured by integrals involving $\kappa_{00'}(t, t')$ and $\kappa_{0'0}(t, t')$. The signal from one auxiliary neuron reaches the other via (at least) disynaptic paths, which have net strength $1/N$. When the N contributions from all paths are summed, a signal of order $1/\sqrt{N}$ arises. Third, neurons 0 and $0'$ have direct connections, $J_{00'}$ and $J_{0'0}$, which have strength $\sim 1/\sqrt{N}$ and induce a covariance of the same order. In weakly coupled networks (i.e., $J_{ij} \sim 1/N$), only this direct-coupling term contributes at leading order. The latter two effects have self-connection counterparts (i.e., $\mu = \nu$ terms) of order $1/\sqrt{N}$ in Eq. 7, but they contribute to the cross-covariance at sub-leading order.

Importantly, the couplings and dynamical variables in these expressions are independent of each other by virtue of the cavity construction. We derive statistics of $\eta_\mu(t)$ and $\kappa_{\mu\nu}(t, t')$ sufficient for determining $\psi_a(\tau, \tau')$ by performing disorder averages over products of these fields, leveraging the independence of the couplings and dynamical variables in Eqs. 8a and 8b. We then enforce self-consistency by noting that the auxiliary pair is statistically equivalent to any reservoir pair, allowing these averages to be expressed through DMFT order parameters. Let $\theta = \{\eta_\mu\} \cup \{\kappa_{\mu\nu}\} \cup \{\mathcal{J}_{\mu\nu}\}$. All variables in θ have mean zero. For $\eta_\mu(t)$,

$$\langle \eta_\mu(t) \eta_\nu(t + \tau) \rangle_\theta = \delta_{\mu\nu} g^2 C_\phi(\tau), \quad (9a)$$

$$\begin{aligned} & \langle \langle \eta_0(t) \eta_{0'}(t + \tau) \rangle_t \langle \eta_0(t') \eta_{0'}(t' + \tau') \rangle_{t'} \rangle_\theta \\ &= \frac{g^4}{N} (C_\phi(\tau) C_\phi(\tau') + \psi_\phi(\tau, \tau')). \end{aligned} \quad (9b)$$

For $\kappa_{\mu\nu}(t, t')$,

$$\begin{aligned} & \langle \langle \kappa_{\mu\nu}(t, t - \tau) \rangle_t \langle \kappa_{\rho\sigma}(t', t' - \tau') \rangle_{t'} \rangle_\theta \\ &= \delta_{\mu\rho} \delta_{\nu\sigma} \frac{g^4}{N} \Gamma(\tau, \tau'), \end{aligned} \quad \text{where} \quad (10a)$$

$$\begin{aligned} \Gamma(\tau, \tau') &= \langle \langle \phi'_0(t) \chi_{00}(t, t - \tau) \rangle_t \langle \phi'_0(t') \chi_{00}(t', t' - \tau') \rangle_{t'} \rangle_\theta \\ &+ N \langle \langle \phi'_0(t) \chi_{00'}(t, t - \tau) \rangle_t \langle \phi'_0(t') \chi_{00'}(t', t' - \tau') \rangle_{t'} \rangle_\theta. \end{aligned} \quad (10b)$$

By causality, $\Gamma(\tau, \tau') = 0$ for $\tau, \tau' < 0$. Eq. 5 gives

$$\psi_a(\tau, \tau') = N \langle \langle a_0(t) a_{0'}(t + \tau) \rangle_t \langle a_0(t') a_{0'}(t' + \tau') \rangle_{t'} \rangle_\theta. \quad (11)$$

Finally, cross-covariances of distinct variables in θ vanish.

Solving the Two-Site DMFT: Full details of the solution are given in the Appendix. We first determine $\Gamma(\tau, \tau')$. Upon computing $\chi_{00}(t, t')$ and $\chi_{00'}(t, t')$ and applying the self-consistency conditions, Eq. 10b becomes

$$\Gamma(\tau, \tau') = \alpha^2 \Theta(\tau) \Theta(\tau') e^{-\tau} e^{-\tau'} (1 + \nu \tau \tau') \quad (12)$$

$$+ \nu^2 \int_{-\infty}^{\tau} du \int_{-\infty}^{\tau'} du' (\tau - u) (\tau' - u') e^{-(\tau - u)} e^{-(\tau' - u')} \Gamma(u, u'),$$

a Volterra equation in $\Gamma(\tau, \tau')$. Solving in Fourier space,

$$\hat{\Gamma}(\omega_1, \omega_2) = \frac{\alpha^2}{2\pi} \frac{1}{(1 + i\omega_1)(1 + i\omega_2) - \nu}. \quad (13)$$

For this to be a valid solution, its inverse transform must vanish for $\tau, \tau' < 0$. Treated as a function over ω_1 , $\hat{\Gamma}(\omega_1, \omega_2)$ has a single pole at $i(1 - \nu/(1 + \omega_2^2))$, which is in the positive imaginary half-plane for all ω_2 since $\nu < 1$. When $\tau < 0$, we compute the inverse transform by taking a contour around the negative imaginary half-plane, so $\Gamma(\tau, \tau')$ indeed vanishes. By symmetry, it also vanishes for $\tau' < 0$.

We next solve for $\psi_a(\tau, \tau')$. It is convenient to determine $\psi_\phi(\tau, \tau')$ first. Using Eq. 11 and the other self-consistency conditions, $\psi_\phi(\tau, \tau')$ can be expressed as a sum of contributions from the three above-described effects generating the cross-covariance between neurons 0 and $0'$, $\psi_\phi(\tau, \tau') = F_\eta(\tau, \tau') + F_\kappa(\tau, \tau') + F_{\mathcal{J}}(\tau, \tau')$, where

$$\begin{aligned} F_\eta(\tau, \tau') &= \frac{\nu^2}{4} \int_{-\infty}^{\infty} du \int_{-\infty}^{\infty} du' e^{-|\tau - u|} e^{-|\tau' - u'|} \\ &\quad \times (C_\phi(u) C_\phi(u') + \psi_\phi(u, u')), \end{aligned} \quad (14a)$$

$$F_\kappa(\tau, \tau') = g^2 \nu \int_{-\infty}^{\infty} du \int_{-\infty}^{\infty} du' \Gamma(u, u') \quad (14b)$$

$$\begin{aligned} & \times (\tilde{C}_\phi(-u + \tau) \tilde{C}_\phi(-u' + \tau') + \tilde{C}_\phi(-u - \tau) \tilde{C}_\phi(-u' - \tau')), \\ F_{\mathcal{J}}(\tau, \tau') &= \nu (\tilde{C}_\phi(\tau) \tilde{C}_\phi(\tau') + \tilde{C}_\phi(-\tau) \tilde{C}_\phi(-\tau')), \end{aligned} \quad (14c)$$

providing a Volterra equation in $\psi_\phi(\tau, \tau')$. Solving in Fourier space recovers Eq. 6 for $a = \phi$. Similar steps recover Eq. 6 for $a = x$.

Effective Dimension: Let $\Sigma_{ij}^a = \langle a_i(t) a_j(t) \rangle_t$ denote the covariance matrix of the a variables and λ_i^a its eigenvalues. Following [29–35, 37, 45, 46], we define the effective dimension as the participation ratio of this spectrum,

$$\text{PR}_a = \frac{1}{N} \frac{(\sum_i \lambda_i^a)^2}{\sum_i (\lambda_i^a)^2}, \quad (15)$$

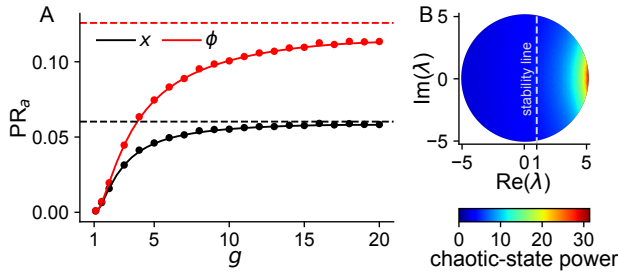


FIG. 2. (A) Effective dimension PR_a for $a \in \{x, \phi\}$. Lines: theory. Dots: simulations of size $N = 2500$. Median values over 50 disorder realizations are shown. (B) Root-mean-square power in the chaotic state for eigenmodes of the stability matrix at the trivial fixed point with $g = 5$. $\phi = \tanh$.

where the factor $1/N$ makes this an intensive quantity, $0 \leq PR_a \leq 1$. PR_a provides a linear notion of dimensionality, corresponding roughly to the minimal dimension, relative to N , of a subspace in which the strange attractor can be embedded with small ℓ^2 distortion. In practice, this embedding subspace can be obtained from data using principal components analysis [45–47]. We evaluate PR_a in the limit $N \rightarrow \infty$ by writing the numerator and denominator of Eq. 15 as the squared trace and Frobenius norm, respectively, of Σ^a , then expressing these quantities using DMFT order parameters, yielding

$$PR_a = \frac{C_a^2(0)}{C_a^2(0) + \psi_a(0,0)}. \quad (16)$$

Evaluating $\psi_a(0,0)$ from Eq. 6 and $C_a(0)$ from the classic DMFT, we find tight agreement between the analytical and simulation-based dimensions (Fig. 2A). PR_a grows monotonically with g as the activity becomes more tempestuous. The fact that $PR_\phi > PR_x$ reflects the dimension-expanding effect of the nonlinearity $\phi(\cdot)$ as has been characterized in feedforward networks [37, 53]. This analysis highlights that the unnormalized effective dimension is extensive, providing the first analytical evidence of extensive chaos in this system [33].

Limit of $g \rightarrow \infty$: We define non-diverging x variables, $\bar{x}_i(t) = x_i(t)/g$, $\bar{C}_x(\tau) = C_x(\tau)/g^2$. In this limit, the Newtonian dynamics for $\bar{C}_x(\tau)$ approach $\partial_\tau^2 \bar{C}_x(\tau) = \bar{C}_x(\tau) - (2/\pi) \arcsin(\bar{C}_x(\tau)/\bar{C}_x(0))$ with $\bar{C}_x(0) = 2(1 - 2/\pi)$ [54] while ν approaches $1/(\pi - 2)$. As PR_a can be expressed in terms of $\bar{C}_x(\tau)$ and ν , both of which saturate, so too does PR_a . The saturating values are $PR_x \approx 6.02\%$ and $PR_\phi \approx 12.6\%$ (Fig. 2A, dashed lines), corresponding to the “Ising limit” of a step-function nonlinearity. The boundedness of the effective dimension substantially below one for arbitrarily large g despite random isotropic couplings is surprising and implies that structured couplings are required to increase the dimension further.

Limit of $g \rightarrow g_{crit}^+$: Henceforth, we assume $\phi = \tanh$, so $g_{crit} = 1$. To first order in $\epsilon = g - 1 \ll 1$, $C_\phi(\tau) = \epsilon \operatorname{sech}(\epsilon\tau/\sqrt{3})$ [54]. Thus, the magnitude of

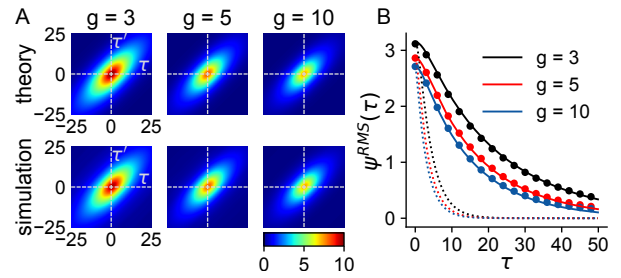


FIG. 3. (A) Order parameter $\psi_\phi(\tau, \tau')$. (B) Typical lag- τ cross-covariance, $\psi_\phi^{\text{RMS}}(\tau)$. Solid lines: theory. Dots: simulations. Dotted lines: rescaled single-neuron autocovariance $C_\phi(\tau)$ for comparison. $N = 2500$. Median values across 50 disorder realizations are shown. $\phi = \tanh$.

activity vanishes as $\sim \sqrt{\epsilon}$ and the timescale diverges as $\sim 1/\epsilon$. Expressing $\nu = 1 - \epsilon^2/3$, $\psi_a(0,0)$ diverges as $\psi_a(0,0) = c/\epsilon$, $c \approx 4.27$. Cross-covariances and cross-correlations have magnitudes of order $1/\sqrt{N\epsilon}$ and $1/\sqrt{N\epsilon^3}$, respectively. Note that a network with ϵ smaller than order $1/N^{1/3}$ cannot admit an asynchronous chaotic state as cross-correlations would be larger than order-one, underscoring that a sharp transition to chaos occurs only in the limit $N \rightarrow \infty$ (for finite N , this transition is punctuated by limit cycles and nonzero fixed points) [1]. Finally, the effective dimension vanishes as $PR_a = \epsilon^3/c$.

Linear Stability Analysis: Stability at the trivial fixed point, $x_i(t) = 0$, is determined by the spectrum of \mathbf{J} , which, in the limit $N \rightarrow \infty$, is a uniform disk of radius g centered at the origin [55, 56]. For $g > 1$, the spectrum protrudes beyond the stability line $Re(\lambda) = 1$, indicating local instability. The fractional area of the spectrum beyond the stability line goes as $\sim \epsilon^{3/2}$. By contrast, $PR_a \sim \epsilon^3 \ll \epsilon^{3/2}$, implying that locally unstable modes contribute to the chaotic state in a nonuniform manner. Indeed, simulations indicate that locally unstable modes with large real part have far greater variance in the chaotic state than those with small real part (Fig. 2B). As ϵ must be of order at least $1/N^{1/3}$ for a chaotic state to exist, the minimal number of locally unstable modes is $\sim N(1/N^{1/3})^{3/2} \sim \sqrt{N}$, suggesting that chaos is possible even when the trivial fixed point is destabilized by a subextensive number of modes.

Temporal Structure of Cross-Covariances: Our focus thus far has been on the effective dimension, expressed via $\psi_a(0,0)$. We now consider $\psi_a(\tau, \tau')$ in full to extract temporal information from the DMFT. The theoretical prediction for $\psi_a(\tau, \tau')$, Eq. 6, displays tight agreement with simulations (Fig. 3A, B). That $\psi_a(\tau, \tau) \neq \psi_a(\tau, -\tau)$ reflects the dissipative, time-irreversible nature of the network. Whereas $C_a(\tau)$ describes the temporal structure of individual neurons, $\psi_a(\tau, \tau')$ describes the temporal structure embedded in correlations between neurons. We define $\psi_a^{\text{RMS}}(\tau) = \sqrt{\psi_a(\tau, \tau)}$, which is \sqrt{N} times the root-mean-square strength of a lag- τ cross-covariance.

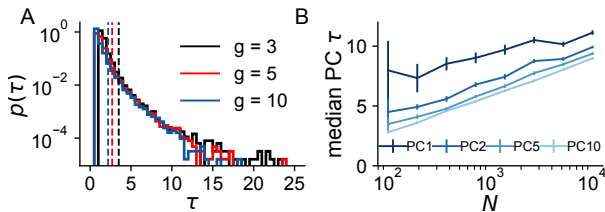


FIG. 4. Timescales of principal components (PCs) of the ϕ variables. **(A)** Density of PC timescales in simulations. Dashed lines: single-neuron timescales. $N = 2500$, 50 disorder realizations. **(B)** Timescales of leading PCs for N spanning two orders of magnitude. $g = 10$. Median timescales across 50 disorder realizations are shown. Error bars: standard error of the mean. Timescales were measured as the full width at half max of the autocovariance. $\phi = \tanh$.

Notably, $\psi_a^{\text{RMS}}(\tau)$ displays a much slower exponential decay than $C_a(\tau)$ (Fig. 3B). As this slow timescale is not present at the level of individual neurons, it must arise in collective activity. This motivated us to examine in simulations the timescales of collective modes obtained by principal components analysis (i.e., by diagonalizing Σ^a and projecting the a variables onto the eigenvectors). The timescales of principal components (PCs) decrease across the variance-ranked PC index, implying that slow modes account for the most variance.

As expected from the slow decay of $\psi_a^{\text{RMS}}(\tau)$, the leading PCs have timescales many times slower than those of individual neurons (Fig. 4A). The density of timescales, $p(\tau)$, is suppressed at small τ such that no PCs have a timescale much less than one, the dimensionless time constant of the dynamics (Eq. 1). At large τ , $p(\tau)$ has an exponential tail. If the exponential form of $p(\tau)$ persists in the limit $N \rightarrow \infty$, the timescales of leading PCs are expected to diverge as $\sim \log N$. By simulating networks with sizes ranging from $\mathcal{O}(10^2)$ to $\mathcal{O}(10^4)$, we confirmed this prediction (Fig. 4B). Prior studies have proposed that structure in synaptic connectivity, e.g., in the form of clusters [2, 57] or partial coupling symmetry [58, 59], is required to generate long timescales. We find that long timescales emerge even in completely unstructured networks, albeit with only a $\log N$ divergence. Moreover, unlike in prior proposals, these slow timescales are not visible within any individual neuron, but arise at the collective level through the temporal structure of cross-covariances to which our theory provides access.

Discussion: We have calculated, for the first time, the structure of time-lagged cross-covariances in a chaotic nonlinear neural network. Prior studies have analyzed cross-covariances in linear models, which do not display rich internal dynamics [32, 35, 60–63]. One output of our calculation is the second moment of the spectral density of the covariance matrix. A more general problem is to compute this density in full, as has been done for linear networks [35]. Another unsolved problem is to compute

the Lyapunov spectrum, which determines the intrinsic dimension of the strange attractor (in contrast to the embedding dimension we have studied) [33]. Several works have rederived the mean-field equations of [1] via path-integral or field-theoretic formalisms [54, 64, 65]. Recapitulating through such a formalism the two-site mean-field equations we have derived could be interesting.

Our work enables analytical investigations of many important questions in neuroscience, machine learning, and statistical physics. The two-site cavity DMFT provides a framework for studying how the dimension of activity is shaped by various forms of structure in \mathbf{J} , such as partial (anti-)symmetry, subpopulations, or low-rank components (see [66–69] for corresponding random-matrix results). For i.i.d. \mathbf{J} , $\psi_a(\tau, \tau')$ depends on only the second moment of the element-wise distribution in analogy with random-matrix results [70]. An important extension will be to incorporate time-dependent inputs, which can shape or suppress chaos [43, 71–73]. In reservoir computing [9–12], the extent to which readout neurons can learn and generalize from a target input-output mapping is likely modulated by the effective dimension of activity in analogy with the feedforward case [37, 74]. Finally, by withholding averages over the auxiliary-pair couplings, our framework enables calculation of the posterior distribution over $J_{\mu\nu}$ conditioned on the pair’s covariance matrix, where the uncertainty in the posterior arises due to the unmeasured reservoir neurons. By extending our calculation to more than two auxiliary neurons, one could compute the posterior over couplings among an intensive subset of neurons conditioned on their covariance matrix, providing a rigorous setting for addressing the problem of inferring synaptic connectivity from recordings of neural activity in sparsely sampled neural circuits [75] and analogous inverse problems in statistical physics [76–78].

ACKNOWLEDGEMENTS

We are very appreciative of Haim Sompolinsky for his advice on this work. We thank Sean Escola, Rainer Engelken, and Samuel Muscinelli for comments on the manuscript. We thank Sean Escola and James Murray for early conversations. The authors were supported by the Gatsby Charitable Foundation and NSF NeuroNex award DBI-1707398. A. L.-K. was also supported by the McKnight Endowment Fund.

-
- [1] H. Sompolinsky, A. Crisanti, and H.-J. Sommers, *Physical Review Letters* **61**, 259 (1988).
 - [2] M. Stern, H. Sompolinsky, and L. F. Abbott, *Physical Review E* **90**, 062710 (2014).

- [3] Y. Bahri, J. Kadmon, J. Pennington, S. S. Schoenholz, J. Sohl-Dickstein, and S. Ganguli, *Annual Review of Condensed Matter Physics* **11** (2020).
- [4] B. Poole, S. Lahiri, M. Raghu, J. Sohl-Dickstein, and S. Ganguli, *Advances in Neural Information Processing Systems* **29** (2016).
- [5] Q. V. Le, N. Jaitly, and G. E. Hinton, arXiv preprint arXiv:1504.00941 (2015).
- [6] S. S. Schoenholz, J. Gilmer, S. Ganguli, and J. Sohl-Dickstein, arXiv preprint arXiv:1611.01232 (2016).
- [7] J. Martens, A. Ballard, G. Desjardins, G. Swirszcz, V. Dalibard, J. Sohl-Dickstein, and S. S. Schoenholz, arXiv preprint arXiv:2110.01765 (2021).
- [8] D. A. Roberts, S. Yaida, and B. Hanin, arXiv preprint arXiv:2106.10165 (2021).
- [9] H. Jaeger and H. Haas, *science* **304**, 78 (2004).
- [10] W. Maass, P. Joshi, and E. D. Sontag, *PLoS Computational Biology* **3**, e165 (2007).
- [11] A. Rivkind and O. Barak, *Physical Review Letters* **118**, 258101 (2017).
- [12] L. Susman, F. Mastrogiuseppe, N. Brenner, and O. Barak, *Physical Review Research* **3**, 013176 (2021).
- [13] F. Mastrogiuseppe and S. Ostojic, *Neuron* **99**, 609 (2018).
- [14] F. Schuessler, F. Mastrogiuseppe, A. Dubreuil, S. Ostojic, and O. Barak, *Advances in Neural Information Processing Systems* **33**, 13352 (2020).
- [15] C. H. Martin and M. W. Mahoney, *J. Mach. Learn. Res.* **22**, 1 (2021).
- [16] A. Arieli, A. Sterkin, A. Grinvald, and A. Aertsen, *Science* **273**, 1868 (1996).
- [17] H. Flyvbjerg, K. Sneppen, and P. Bak, *Physical Review Letters* **71**, 4087 (1993).
- [18] S. Ciuchi, F. De Pasquale, and B. Spagnolo, *Physical Review E* **54**, 706 (1996).
- [19] H. Aoki, N. Tsuji, M. Eckstein, M. Kollar, T. Oka, and P. Werner, *Reviews of Modern Physics* **86**, 779 (2014).
- [20] J. Kadmon and H. Sompolinsky, *Physical Review X* **5**, 041030 (2015).
- [21] J. Aljadeff, M. Stern, and T. Sharpee, *Physical Review Letters* **114**, 088101 (2015).
- [22] M. Chen, J. Pennington, and S. Schoenholz, in *International Conference on Machine Learning* (PMLR, 2018) pp. 873–882.
- [23] F. Roy, G. Biroli, G. Bunin, and C. Cammarota, *Journal of Physics A: Mathematical and Theoretical* **52**, 484001 (2019).
- [24] F. Mignacco, F. Krzakala, P. Urbani, and L. Zdeborová, *Advances in Neural Information Processing Systems* **33**, 9540 (2020).
- [25] C. Keup, T. Kühn, D. Dahmen, and M. Helias, *Physical Review X* **11**, 021064 (2021).
- [26] A. van Meegen, T. Kühn, and M. Helias, *Physical Review Letters* **127**, 158302 (2021).
- [27] K. Krishnamurthy, T. Can, and D. J. Schwab, *Physical Review X* **12**, 011011 (2022).
- [28] E. De Giuli and C. Scalliet, arXiv preprint arXiv:2205.02204 (2022).
- [29] K. Rajan, L. Abbott, and H. Sompolinsky, *Advances in Neural Information Processing Systems* **23** (2010).
- [30] L. Abbott, K. Rajan, and H. Sompolinsky, in *The dynamic brain: an exploration of neuronal variability and its functional significance*, edited by M. Ding and D. Glanzman (Oxford University Press, 2011) p. 65–82.
- [31] H. Huang, *Physical Review E* **98**, 062313 (2018).
- [32] S. Recanatesi, G. K. Ocker, M. A. Buice, and E. Shea-Brown, *PLoS Computational Biology* **15**, e1006446 (2019).
- [33] R. Engelken, F. Wolf, and L. Abbott, arXiv preprint arXiv:2006.02427 (2020).
- [34] S. Recanatesi, S. Bradde, V. Balasubramanian, N. A. Steinmetz, and E. Shea-Brown, *bioRxiv* (2020).
- [35] Y. Hu and H. Sompolinsky, *PLoS Computational Biology* **18**, 1 (2022).
- [36] M. Jazayeri and S. Ostojic, *Current opinion in neurobiology* **70**, 113 (2021).
- [37] A. Litwin-Kumar, K. D. Harris, R. Axel, H. Sompolinsky, and L. Abbott, *Neuron* **93**, 1153 (2017).
- [38] S. Chung, D. D. Lee, and H. Sompolinsky, *Physical Review X* **8**, 031003 (2018).
- [39] U. Cohen, S. Chung, D. D. Lee, and H. Sompolinsky, *Nature Communications* **11**, 1 (2020).
- [40] M. Farrell, S. Recanatesi, T. Moore, G. Lajoie, and E. Shea-Brown, *Nature Machine Intelligence* , 1 (2022).
- [41] B. Sorscher, S. Ganguli, and H. Sompolinsky, *bioRxiv* (2021).
- [42] U. Cohen and H. Sompolinsky, arXiv preprint arXiv:2203.07040 (2022).
- [43] D. Sussillo and L. Abbott, *Neuron* **63**, 544 (2009).
- [44] S. Ganguli, H. Sompolinsky, *et al.*, *Annual Review of Neuroscience* **35**, 485 (2012).
- [45] P. Gao and S. Ganguli, *Current Opinion in Neurobiology* **32**, 148 (2015).
- [46] P. Gao, E. Trautmann, B. Yu, G. Santhanam, S. Ryu, K. Shenoy, and S. Ganguli, *bioRxiv* , 214262 (2017).
- [47] E. M. Trautmann, S. D. Stavisky, S. Lahiri, K. C. Ames, M. T. Kaufman, D. J. O’Shea, S. Vyas, X. Sun, S. I. Ryu, S. Ganguli, *et al.*, *Neuron* **103**, 292 (2019).
- [48] R. Price, *IRE Transactions on Information Theory* **4**, 69 (1958).
- [49] M. Mézard, G. Parisi, and M. A. Virasoro, *Spin glass theory and beyond: An Introduction to the Replica Method and Its Applications*, Vol. 9 (World Scientific Publishing Company, 1987).
- [50] M. Advani, S. Lahiri, and S. Ganguli, *Journal of Statistical Mechanics: Theory and Experiment* **2013**, P03014 (2013).
- [51] E. Agoritsas, G. Biroli, P. Urbani, and F. Zamponi, *Journal of Physics A: Mathematical and Theoretical* **51**, 085002 (2018).
- [52] See Mézard *et al.* [49] Ch. V.3 for a two-site cavity approach to spin glasses.
- [53] B. Babadi and H. Sompolinsky, *Neuron* **83**, 1213 (2014).
- [54] A. Crisanti and H. Sompolinsky, *Physical Review E* **98**, 062120 (2018).
- [55] V. L. Girko, *Theory of Probability & Its Applications* **29**, 694 (1985).
- [56] T. Tao and V. Vu, *Communications in Contemporary Mathematics* **10**, 261 (2008).
- [57] A. Litwin-Kumar and B. Doiron, *Nature Neuroscience* **15**, 1498 (2012).
- [58] D. Martí, N. Brunel, and S. Ostojic, *Physical Review E* **97**, 062314 (2018).
- [59] K. Berlemont and G. Mongillo, *bioRxiv* (2022).
- [60] I. Ginzburg and H. Sompolinsky, *Physical review E* **50**, 3171 (1994).
- [61] D. Grytskyy, T. Tetzlaff, M. Diesmann, and M. Helias, *Frontiers in Computational Neuroscience* **7**, 131 (2013).

- [62] D. Dahmen, S. Grün, M. Diesmann, and M. Helias, Proceedings of the National Academy of Sciences **116**, 13051 (2019).
- [63] Y.-L. Shi, R. Zeraati, A. Levina, and T. A. Engel, arXiv preprint arXiv:2207.07930 (2022).
- [64] K. Segadlo, B. Epping, A. van Meegen, D. Dahmen, M. Krämer, and M. Helias, arXiv preprint arXiv:2112.05589 (2021).
- [65] K. Grosvenor and R. Jefferson, SciPost Physics **12**, 081 (2022).
- [66] H. J. Sommers, A. Crisanti, H. Sompolinsky, and Y. Stein, Physical Review Letters **60**, 1895 (1988).
- [67] K. Rajan and L. Abbott, Physical Review Letters **97**, 188104 (2006).
- [68] T. Tao, Probability Theory and Related Fields **155**, 231 (2013).
- [69] J. Aljadeff, D. Renfrew, and M. Stern, Journal of Mathematical Physics **56**, 103502 (2015).
- [70] T. Tao and V. Vu, Acta mathematica **206**, 127 (2011).
- [71] L. Molgedey, J. Schuchhardt, and H. G. Schuster, Physical Review Letters **69**, 3717 (1992).
- [72] K. Rajan, L. Abbott, and H. Sompolinsky, Physical Review E **82**, 011903 (2010).
- [73] J. Schuecker, S. Goedeke, and M. Helias, Physical Review X **8**, 041029 (2018).
- [74] M. Rigotti, O. Barak, M. R. Warden, X.-J. Wang, N. D. Daw, E. K. Miller, and S. Fusi, Nature **497**, 585 (2013).
- [75] A. Das and I. R. Fiete, Nature Neuroscience **23**, 1286 (2020).
- [76] J. Sohl-Dickstein, P. B. Battaglino, and M. R. DeWeese, Physical Review Letters **107**, 220601 (2011).
- [77] M. Castellana and W. Bialek, Physical Review Letters **113**, 117204 (2014).
- [78] V. Ngampruetikorn, V. Sachdeva, J. Torrence, J. Humpalik, D. J. Schwab, and S. E. Palmer, Physical Review Research **4**, 023240 (2022).

Appendix for “Dimension of Activity in Random Neural Networks”

Here, we explain the solution of the two-site DMFT in more detail. The solution uses the two-dimensional mean-field dynamics (Eq. 7) in conjunction with the self-consistency conditions (Eqs. 9, 10, and 11). We first review two relations involving correlated Gaussian variables that will be used later on.

Gaussian Relations

The first relation is Price’s theorem. Let x and y denote zero-mean, jointly Gaussian variables with identical variance α and covariance β . Let $f(\cdot)$ denote a scalar function (for our purposes, this will be the sigmoid-shaped nonlinearity $\phi(\cdot)$, but we keep it general here). Price’s theorem is the statement that

$$\partial_{\beta}^n \langle f(x)f(y) \rangle_{x,y} = \left\langle f^{(n)}(x)f^{(n)}(y) \right\rangle_{x,y}. \quad (17)$$

In particular,

$$\partial_{\beta}^n \langle f(x)f(y) \rangle_{x,y} \Big|_{\beta=0} = \left\langle f^{(n)}(x) \right\rangle_x^2. \quad (18)$$

It follows that the Taylor expansion of $\langle f(x)f(y) \rangle_{x,y}$ about $\beta = 0$ is

$$\langle f(x)f(y) \rangle_{x,y} = \langle f(x) \rangle_x^2 + \langle f'(x) \rangle_x^2 \beta + \frac{1}{2!} \langle f''(x) \rangle_x^2 \beta^2 + \dots \quad (19)$$

When f is an odd function, terms with even powers of β are zero, so the first term in the Taylor series is $\langle f'(x) \rangle_x^2 \beta$. The second relation is

$$\langle f(x)y \rangle_{x,y} = \langle f'(x) \rangle_x \beta, \quad (20)$$

which is exact and can be proved via integration by parts.

Solving the Two-Site DMFT

We first note a couple of conventions. Throughout, we use the Fourier transform

$$\hat{f}(\omega) = \frac{1}{(2\pi)^{\frac{n}{2}}} \int_{-\infty}^{\infty} d^n t e^{-i\omega^T t} f(\mathbf{t}), \quad (21)$$

where $\mathbf{t}, \boldsymbol{\omega} \in \mathbb{R}^n$. For clarity, we forgo the Greek-index notation in favor of writing separate equations for each of the auxiliary-neuron indices, 0 and 0' (though this has the effect of making the equations appear superficially more dense).

The two-dimensional mean-field dynamics are (reproduced from Eq. 7)

$$(1 + \partial_t)x_0(t) = \eta_0(t) + \frac{1}{\sqrt{N}} \left[\int_{-\infty}^t dt' \kappa_{00}(t, t') \phi_0(t') + \int_{-\infty}^t dt' \kappa_{00'}(t, t') \phi_{0'}(t') + \mathcal{J}_{00} \phi_0(t) + \mathcal{J}_{00'} \phi_{0'}(t) \right], \quad (22a)$$

$$(1 + \partial_t)x_{0'}(t) = \eta_{0'}(t) + \frac{1}{\sqrt{N}} \left[\int_{-\infty}^t dt' \kappa_{0'0}(t, t') \phi_0(t') + \int_{-\infty}^t dt' \kappa_{0'0'}(t, t') \phi_{0'}(t') + \mathcal{J}_{0'0} \phi_0(t) + \mathcal{J}_{0'0'} \phi_{0'}(t) \right]. \quad (22b)$$

We ultimately want to determine $\psi_a(\tau, \tau')$. As stated in the main text, we first determine $\Gamma(\tau, \tau')$, which encodes the second-order statistics of the two-dimensional random field $\kappa_{\mu\nu}(t, t')$. This is accomplished by evaluating and solving Eq. 10b. We determine $\Gamma(\tau, \tau')$ first because its solution does not require $\psi_a(\tau, \tau')$, whereas solving for $\psi_a(\tau, \tau')$ requires $\Gamma(\tau, \tau')$.

Solving for $\Gamma(\tau, \tau')$

Toward evaluating Eq. 10b, we compute the on- and off-diagonal linear susceptibilities, $\chi_{00}(t, t')$ and $\chi_{00'}(t, t')$, using Eq. 22. To compute $\chi_{00}(t, t')$, we add a delta-function input, $\epsilon \delta(t - t')$, to neuron 0. We then compute the perturbation $\Delta x_0(t)$ to $x_0(t)$ under this input. Then, $\chi_{00}(t, t') = \lim_{\epsilon \rightarrow 0} \Delta x_0(t)/\epsilon$. $\chi_{00'}(t, t')$ is computed in the same way, only the delta-function input is added to neuron 0'. We compute $\chi_{00}(t, t')$ to order one and $\chi_{00'}(t, t')$ to order $1/\sqrt{N}$ (which is to leading order in both cases). It is helpful to integrate Eq. 22,

$$x_0(t) = \tilde{\eta}_0(t) + \frac{1}{\sqrt{N}} \int_{-\infty}^t ds e^{-(t-s)} \left[\int_{-\infty}^s ds' \kappa_{00}(s, s') \phi_0(s') + \int_{-\infty}^s ds' \kappa_{00'}(s, s') \phi_{0'}(s') + \mathcal{J}_{00} \phi_0(s) + \mathcal{J}_{00'} \phi_{0'}(s) \right], \quad (23a)$$

$$x_{0'}(t) = \tilde{\eta}_{0'}(t) + \frac{1}{\sqrt{N}} \int_{-\infty}^t ds e^{-(t-s)} \left[\int_{-\infty}^s ds' \kappa_{0'0}(s, s') \phi_0(s') + \int_{-\infty}^s ds' \kappa_{0'0'}(s, s') \phi_{0'}(s') + \mathcal{J}_{0'0} \phi_0(s) + \mathcal{J}_{0'0'} \phi_{0'}(s) \right] \quad (23b)$$

where $\tilde{\eta}_0(t)$ and $\tilde{\eta}_{0'}(t)$ are low-pass filtered versions of the original fields,

$$\tilde{\eta}_0(t) = \int_{-\infty}^t dt' e^{-(t-t')} \eta_0(t'), \quad \tilde{\eta}_{0'}(t) = \int_{-\infty}^t dt' e^{-(t-t')} \eta_{0'}(t'). \quad (24)$$

To compute $\chi_{00}(t, t')$, we add the delta-function input to neuron 0, which results in the term $\epsilon \Theta(t - t') e^{-(t-t')}$ being added to the right-hand side of Eq. 23a. Only the direct input of the delta function to neuron 0 contributes to $\chi_{00}(t, t')$ at order one. The self-feedback path $0 \rightarrow 0$ contributes at order $1/\sqrt{N}$ while feedback through the indirect path $0 \rightarrow 0' \rightarrow 0$ contributes at order $1/N$. Thus,

$$\chi_{00}(t, t') = \Theta(t - t') e^{-(t-t')}. \quad (25)$$

To compute $\chi_{00'}(t, t')$, we add the delta-function input to neuron 0', which results in the term $\epsilon \Theta(t - t') e^{-(t-t')}$ being added to the right-hand side of Eq. 23b. Only the path $0' \rightarrow 0$ contributes to $\chi_{00'}(t, t')$ at leading order, $1/\sqrt{N}$. The path $0' \rightarrow 0 \rightarrow 0$ contributes at order $1/N$, while $0' \rightarrow 0 \rightarrow 0' \rightarrow 0$ contributes at order $1/N^2$, and so on. Thus,

$$\chi_{00'}(t, t') = \frac{1}{\sqrt{N}} \Theta(t - t') e^{-(t-t')} \left[\int_{t'}^t ds \int_{t'}^s ds' e^{s-s'} \kappa_{00'}(s, s') \phi_{0'}(s') + \mathcal{J}_{00'} \int_{t'}^t ds \phi_{0'}(s) \right], \quad (26)$$

where $\phi_{\mu}'(t) = \phi'(x_{\mu}(t))$. To facilitate averaging over t , we rewrite these expressions for $\chi_{00}(t, t')$ and $\chi_{00'}(t, t')$ as

$$\chi_{00}(t, t - \tau) = \Theta(\tau) e^{-\tau}, \quad (27)$$

$$\chi_{00'}(t, t - \tau) = \frac{1}{\sqrt{N}} \Theta(\tau) e^{-\tau} \left[\int_0^{\tau} ds \int_0^s ds' e^{s-s'} \kappa_{00'}(s + t - \tau, s' + t - \tau) \phi_{0'}(s' + t - \tau) + \mathcal{J}_{00'} \int_0^{\tau} ds \phi_{0'}(s + t - \tau) \right] \quad (28)$$

We are now equipped to evaluate Eq. 10b for $\Gamma(\tau, \tau')$. This requires evaluating two temporal averages. The first is

$$\langle \phi_{0'}'(t) \chi_{00}(t, t - \tau) \rangle_t = \alpha \Theta(\tau) e^{-\tau}. \quad (29)$$

The second is $\langle \phi'_0(t)\chi_{00'}(t, t - \tau) \rangle_t$. To evaluate this term, note that, to leading order (order one),

$$\langle \phi'_0(t)\phi'_{0'}(s' + t - \tau)\kappa_{00'}(s + t - \tau, s' + t - \tau) \rangle_t = \alpha^2 \langle \kappa_{00'}(t, t - (s - s')) \rangle_t, \quad (30)$$

$$\langle \phi'_0(t)\phi'_{0'}(s + t - \tau) \rangle_t = \alpha^2, \quad (31)$$

where we have noted that the pairwise temporal covariances between all pairs of these terms vanish for $N \rightarrow \infty$. This allows us to evaluate the temporal average of interest to order leading order, $1/\sqrt{N}$,

$$\langle \phi'_0(t)\chi_{00'}(t, t - \tau) \rangle_t = \frac{1}{\sqrt{N}}\Theta(\tau)e^{-\tau} \left[\alpha^2 \int_0^\tau ds \int_0^s ds' e^{s-s'} \langle \kappa_{00'}(t, t - (s - s')) \rangle_t + \mathcal{J}_{00'}\alpha^2\tau \right]. \quad (32)$$

Applying a change of coordinates to the double integral in this expression gives

$$\langle \phi'_0(t)\chi_{00'}(t, t - \tau) \rangle_t = \frac{1}{\sqrt{N}}\Theta(\tau) \left[\alpha^2 \int_0^\tau du e^{-(\tau-u)} (\tau - u) \langle \kappa_{00'}(t, t - u) \rangle_t + \mathcal{J}_{00'}\alpha^2\tau \right]. \quad (33)$$

It is now straightforward to evaluate Eq. 10b by performing the averages over θ and applying the self-consistency conditions. This yields

$$\begin{aligned} \Gamma(\tau, \tau') = \alpha^2\Theta(\tau)\Theta(\tau')e^{-\tau}e^{-\tau'} + g^4\alpha^4\Theta(\tau)\Theta(\tau') \int_0^\tau du \int_0^{\tau'} du' e^{-(\tau-u)}e^{-(\tau'-u')} (\tau - u)(\tau' - u')\Gamma(u, u') \\ + g^2\alpha^4\Theta(\tau)\Theta(\tau')\tau\tau'. \end{aligned} \quad (34)$$

We apply the definition $\nu = g^2\alpha^2$ in several places. We extend the lower limits of the integrals to $-\infty$ because $\Gamma(u, u')$ vanishes for $u, u' < 0$ (an important check of self-consistency is that the resulting solution indeed vanishes in this regime). We therefore arrive at the equation (reproduced from Eq. 12)

$$\Gamma(\tau, \tau') = \alpha^2\Theta(\tau)\Theta(\tau')e^{-\tau}e^{-\tau'} (1 + \nu\tau\tau') + \nu^2 \int_{-\infty}^\tau du \int_{-\infty}^{\tau'} du' (\tau - u)(\tau' - u')e^{-(\tau-u)}e^{-(\tau'-u')}\Gamma(u, u'). \quad (35)$$

Performing a Fourier transform gives

$$\hat{\Gamma}(\omega_1, \omega_2) = \frac{\alpha^2}{2\pi(1 + i\omega_1)(1 + i\omega_2)} + \frac{\alpha^2\nu}{2\pi(1 + i\omega_1)^2(1 + i\omega_2)^2} + \frac{\nu^2}{(1 + i\omega_1)^2(1 + i\omega_2)^2}\hat{\Gamma}(\omega_1, \omega_2), \quad (36)$$

which can be solved to give (reproduced from Eq. 13)

$$\hat{\Gamma}(\omega_1, \omega_2) = \frac{\alpha^2}{2\pi} \frac{1}{(1 + i\omega_1)(1 + i\omega_2) - \nu}. \quad (37)$$

In the main text, we show that the inverse transform vanishes for $\tau, \tau' < 0$ if, and only if, $\nu < 1$. The condition $\nu < 1$ is guaranteed by the Mexican-hat shape of the Newtonian potential (the potential has negative curvature at the origin, and ν is one plus this curvature).

Solving for $\psi_\phi(\tau, \tau')$

With the solution for $\Gamma(\tau, \tau')$ in hand, we now determine $\psi_\phi(\tau, \tau')$. We determine $\psi_\phi(\tau, \tau')$ before $\psi_x(\tau, \tau')$ as the solution to the former does not depend on the latter, but the reverse is not true. We first rewrite the integrated

mean-field dynamics of Eq. 23 to facilitate averaging over t ,

$$x_0(t) = \tilde{\eta}_0(t) + \frac{1}{\sqrt{N}} \int_0^\infty ds e^{-s} \left[\int_0^\infty ds' \kappa_{00}(t-s, t-s-s') \phi_0(t-s-s') \right. \\ \left. + \int_0^\infty ds' \kappa_{00'}(t-s, t-s-s') \phi_{0'}(t-s-s') \right. \\ \left. + \mathcal{J}_{00} \phi_0(t-s) + \mathcal{J}_{00'} \phi_{0'}(t-s) \right], \quad (38a)$$

$$x_{0'}(t) = \tilde{\eta}_{0'}(t) + \frac{1}{\sqrt{N}} \int_0^\infty ds e^{-s} \left[\int_0^\infty ds' \kappa_{0'0}(t-s, t-s-s') \phi_0(t-s-s') \right. \\ \left. + \int_0^\infty ds' \kappa_{0'0'}(t-s, t-s-s') \phi_{0'}(t-s-s') \right. \\ \left. + \mathcal{J}_{0'0} \phi_0(t-s) + \mathcal{J}_{0'0'} \phi_{0'}(t-s) \right]. \quad (38b)$$

Applying the nonlinearity $\phi(\cdot)$ to both sides and performing a first-order Taylor expansion gives

$$\phi_0(t) = \phi(\tilde{\eta}_0(t)) + \frac{1}{\sqrt{N}} \phi'(\tilde{\eta}_0(t)) \int_0^\infty ds e^{-s} \left[\int_0^\infty ds' \kappa_{00}(t-s, t-s-s') \phi_0(t-s-s') \right. \\ \left. + \int_0^\infty ds' \kappa_{00'}(t-s, t-s-s') \phi_{0'}(t-s-s') \right. \\ \left. + \mathcal{J}_{00} \phi_0(t-s) + \mathcal{J}_{00'} \phi_{0'}(t-s) \right], \quad (39)$$

$$\phi_{0'}(t) = \phi(\tilde{\eta}_{0'}(t)) + \frac{1}{\sqrt{N}} \phi'(\tilde{\eta}_{0'}(t)) \int_0^\infty ds e^{-s} \left[\int_0^\infty ds' \kappa_{0'0}(t-s, t-s-s') \phi_0(t-s-s') \right. \\ \left. + \int_0^\infty ds' \kappa_{0'0'}(t-s, t-s-s') \phi_{0'}(t-s-s') \right. \\ \left. + \mathcal{J}_{0'0} \phi_0(t-s) + \mathcal{J}_{0'0'} \phi_{0'}(t-s) \right]. \quad (40)$$

We now compute the temporal average $\langle \phi_0(t) \phi_{0'}(t+\tau) \rangle_t$ to leading order, $1/\sqrt{N}$. To this end, we evaluate several cross terms to leading order (order one),

$$\langle \phi(\tilde{\eta}_0(t)) \phi'(\tilde{\eta}_{0'}(t+\tau)) \kappa_{0'0}(t+\tau-s, t+\tau-s-s') \phi_0(t+\tau-s-s') \rangle_t = \alpha \langle \kappa_{0'0}(t, t-s') \rangle_t C_\phi(-\tau+s+s'), \quad (41a)$$

$$\langle \phi(\tilde{\eta}_{0'}(t+\tau)) \phi'(\tilde{\eta}_0(t)) \kappa_{00'}(t-s, t-s-s') \phi_{0'}(t-s-s') \rangle_t = \alpha \langle \kappa_{00'}(t, t-s') \rangle_t C_\phi(\tau+s+s'), \quad (41b)$$

$$\langle \phi(\tilde{\eta}_0(t)) \phi_0(t+\tau-s) \rangle_t = C_\phi(-\tau+s), \quad (41c)$$

$$\langle \phi(\tilde{\eta}_{0'}(t+\tau)) \phi_{0'}(t-s) \rangle_t = C_\phi(\tau+s). \quad (41d)$$

Now, note that for given realizations, the fields $\eta_0(t)$ and $\eta_{0'}(t)$ are jointly Gaussian in time to leading order, $1/\sqrt{N}$. In particular, $\eta_0(t)$ and $\eta_{0'}(t)$ have a temporal cross-covariance of order $1/\sqrt{N}$, as per Eq. 9, and higher-order temporal cumulants scale as larger powers of $1/N$. Thus, they can be taken to be jointly Gaussian in time within the order- $1/\sqrt{N}$ corrections we consider. This allows us to apply Price's theorem to evaluate

$$\langle \phi(\tilde{\eta}_0(t)) \phi(\tilde{\eta}_{0'}(t+\tau)) \rangle_t = \alpha^2 \langle \tilde{\eta}_0(t) \tilde{\eta}_{0'}(t+\tau) \rangle_t. \quad (42)$$

We can further express the temporal average on the right-hand side as

$$\langle \tilde{\eta}_0(t) \tilde{\eta}_{0'}(t+\tau) \rangle_t = \frac{1}{2} \int_{-\infty}^\infty d\gamma e^{-|\tau-\gamma|} \langle \eta_0(t) \eta_{0'}(t+\tau) \rangle_t. \quad (43)$$

The remaining cross terms that constitute $\langle \phi_0(t) \phi_{0'}(t+\tau) \rangle_t$ are subdominant. Thus,

$$\langle \phi_0(t) \phi_{0'}(t+\tau) \rangle_t = \frac{\alpha^2}{2} \int_{-\infty}^\infty d\gamma e^{-|\tau-\gamma|} \langle \eta_0(t) \eta_{0'}(t+\tau) \rangle_t \\ + \frac{\alpha}{\sqrt{N}} \left[\int_0^\infty ds' \langle \kappa_{0'0}(t, t-s') \rangle_t \tilde{C}_\phi(-\tau+s') + \int_0^\infty ds' \langle \kappa_{00'}(t, t-s') \rangle_t \tilde{C}_\phi(\tau+s') + \mathcal{J}_{0'0} \tilde{C}_\phi(-\tau) + \mathcal{J}_{00'} \tilde{C}_\phi(\tau) \right], \quad (44)$$

where $\tilde{C}_\phi(\tau)$ is a low-pass filtered version of $C_\phi(\tau)$,

$$\tilde{C}_\phi(\tau) = \int_{-\infty}^{\tau} d\gamma e^{-(\tau-\gamma)} C_\phi(\gamma). \quad (45)$$

All that is left in computing $\psi_\phi(\tau, \tau')$ is to square the above expression, average over θ (applying the self-consistency conditions given in the main text), and multiply by N . This gives

$$\begin{aligned} \psi_\phi(\tau, \tau') &= \frac{\alpha^4 g^4}{4} \int_{-\infty}^{\infty} d\gamma \int_{-\infty}^{\infty} d\gamma' e^{-|\tau-\gamma|} e^{-|\tau'-\gamma'|} (C_\phi(\tau) C_\phi(\tau') + \psi_\phi(\tau, \tau')) \\ &\quad + \alpha^2 g^4 \int_0^{\infty} du \int_0^{\infty} du' \Gamma(u, u') \left(\tilde{C}_\phi(-\tau - u) \tilde{C}_\phi(-\tau' - u') + \tilde{C}_\phi(\tau - u) \tilde{C}_\phi(\tau' - u') \right) \\ &\quad + \alpha^2 g^2 \left(\tilde{C}_\phi(-\tau) \tilde{C}_\phi(-\tau') + \tilde{C}_\phi(\tau) \tilde{C}_\phi(\tau') \right). \end{aligned} \quad (46)$$

Since $\Gamma(u, u')$ vanishes for $u, u' < 0$, we can extend the lower limits of the double integral involving $\Gamma(u, u')$ to $-\infty$ to obtain

$$\begin{aligned} \psi_\phi(\tau, \tau') &= \frac{\alpha^4 g^4}{4} \int_{-\infty}^{\infty} d\gamma \int_{-\infty}^{\infty} d\gamma' e^{-|\tau-\gamma|} e^{-|\tau'-\gamma'|} (C_\phi(\tau) C_\phi(\tau') + \psi_\phi(\tau, \tau')) \\ &\quad + \alpha^2 g^2 \int_{-\infty}^{\infty} du \int_{-\infty}^{\infty} du' (g^2 \Gamma(u, u') + \delta(u) \delta(u')) \left(\tilde{C}_\phi(-\tau - u) \tilde{C}_\phi(-\tau' - u') + \tilde{C}_\phi(\tau - u) \tilde{C}_\phi(\tau' - u') \right). \end{aligned} \quad (47)$$

Performing a Fourier transform gives

$$\hat{\psi}_\phi(\tau, \tau') = \nu^2 \frac{\hat{C}_\phi(\omega_1) \hat{C}_\phi(\omega_2) + \hat{\psi}_\phi(\omega_1, \omega_2)}{(1 + \omega_1^2)(1 + \omega_2^2)} + 2\nu \text{Re} \left\{ \left(2\pi g^2 \hat{\Gamma}(\omega_1, \omega_2) + 1 \right) \frac{1}{(1 + i\omega_1)(1 + i\omega_2)} \right\} \hat{C}_\phi(\omega_1) \hat{C}_\phi(\omega_2). \quad (48)$$

Using the Fourier-space solution for $\hat{\Gamma}(\omega_1, \omega_2)$, Eq. 37, we have

$$\left(2\pi g^2 \hat{\Gamma}(\omega_1, \omega_2) + 1 \right) \frac{1}{(1 + i\omega_1)(1 + i\omega_2)} = \frac{1}{(1 + i\omega_1)(1 + i\omega_2) - \nu}. \quad (49)$$

We can now solve Eq. 48 to obtain

$$\hat{\psi}_\phi(\omega_1, \omega_2) = \alpha^4 \left[1 + \frac{\nu^2}{(1 + \omega_1^2)(1 + \omega_2^2) - \nu^2} \right] \left[1 + 2\text{Re} \left\{ \frac{1}{(1 + i\omega_1)(1 + i\omega_2) - \nu} \right\} \frac{(1 + \omega_1^2)(1 + \omega_2^2)}{\nu} \right] \hat{C}_x(\omega_1) \hat{C}_x(\omega_2), \quad (50)$$

where we used $(1 + \omega^2) \hat{C}_x(\omega) = g^2 \hat{C}_\phi(\omega)$, the Fourier-space version of the relation $(1 - \partial_\tau^2) C_x(\tau) = g^2 C_\phi(\tau)$ from the existing mean-field theory. This recovers the central result of the main text, Eq. 6, for $a = \phi$.

Solving for $\psi_x(\tau, \tau')$

We now compute $\psi_x(\tau, \tau')$, following many of the steps performed above. Starting from Eq. 38, we compute the temporal average $\langle x_0(t) x_{0'}(t + \tau) \rangle_t$. To this end, we evaluate several cross terms to leading order (order one),

$$\langle \tilde{\eta}_0(t) \kappa_{0'0}(t + \tau - s, t + \tau - s - s') \phi_0(t + \tau - s - s') \rangle = \alpha \langle \kappa_{0'0}(t, t - s') \rangle_t C_x(-\tau + s + s'), \quad (51a)$$

$$\langle \tilde{\eta}_{0'}(t + \tau) \kappa_{00'}(t - s, t - s - s') \phi_{0'}(t - s - s') \rangle = \alpha \langle \kappa_{00'}(t, t - s') \rangle_t C_x(\tau + s + s'), \quad (51b)$$

$$\langle \tilde{\eta}_0(t) \phi_0(t + \tau - s) \rangle_t = \alpha C_x(-\tau + s), \quad (51c)$$

$$\langle \tilde{\eta}_{0'}(t + \tau) \phi_{0'}(t - s) \rangle_t = \alpha C_x(\tau + s), \quad (51d)$$

where we used the relation Eq. 20 for Gaussian variables. We rewrite $\langle \tilde{\eta}_0(t) \tilde{\eta}_{0'}(t + \tau) \rangle_t$ using Eq. 43. The remaining cross-terms are subdominant. Thus we have

$$\begin{aligned} \langle x_0(t) x_{0'}(t + \tau) \rangle_t &= \frac{1}{2} \int_{-\infty}^{\infty} d\gamma e^{-|\tau-\gamma|} \langle \eta_0(t) \eta_{0'}(t + \tau) \rangle_t \\ &\quad + \frac{\alpha}{\sqrt{N}} \left[\int_0^{\infty} ds' \langle \kappa_{0'0}(t, t - s') \rangle_t \tilde{C}_x(-\tau + s') + \int_0^{\infty} ds' \langle \kappa_{00'}(t, t - s') \rangle_t \tilde{C}_x(\tau + s') + \mathcal{J}_{0'0} \tilde{C}_x(-\tau) + \mathcal{J}_{00'} \tilde{C}_x(\tau) \right]. \end{aligned} \quad (52)$$

As before, we square the above expression, average over θ , and multiply by N . This gives

$$\begin{aligned} \psi_x(\tau, \tau') &= \frac{g^4}{4} \int_{-\infty}^{\infty} d\gamma \int_{-\infty}^{\infty} d\gamma' e^{-|\tau-\gamma|} e^{-|\tau'-\gamma'|} (C_\phi(\tau)C_\phi(\tau') + \psi_\phi(\tau, \tau')) \\ &\quad + \alpha^2 g^4 \int_0^{\infty} du \int_0^{\infty} du' \Gamma(u, u') \left(\tilde{C}_x(-\tau - u) \tilde{C}_x(-\tau' - u') + \tilde{C}_x(\tau - u) \tilde{C}_x(\tau' - u') \right) \\ &\quad + \alpha^2 g^2 \left(\tilde{C}_x(-\tau) \tilde{C}_x(-\tau') + \tilde{C}_x(\tau) \tilde{C}_x(\tau') \right). \end{aligned} \quad (53)$$

Extending the lower limits of the double integral over $\Gamma(u, u')$ gives

$$\begin{aligned} \psi_x(\tau, \tau') &= \frac{g^4}{4} \int_{-\infty}^{\infty} d\gamma \int_{-\infty}^{\infty} d\gamma' e^{-|\tau-\gamma|} e^{-|\tau'-\gamma'|} (C_\phi(\tau)C_\phi(\tau') + \psi_\phi(\tau, \tau')) \\ &\quad + \alpha^2 g^2 \int_{-\infty}^{\infty} du \int_{-\infty}^{\infty} du' (g^2 \Gamma(u, u') + \delta(u)\delta(u')) \left(\tilde{C}_x(-\tau - u) \tilde{C}_x(-\tau' - u') + \tilde{C}_x(\tau - u) \tilde{C}_x(\tau' - u') \right). \end{aligned} \quad (54)$$

We use $\nu = g^2 \alpha^2$ in several places. Performing a Fourier transform gives

$$\hat{\psi}_x(\tau, \tau') = g^4 \frac{\hat{C}_\phi(\omega_1) \hat{C}_\phi(\omega_2) + \hat{\psi}_\phi(\omega_1, \omega_2)}{(1 + \omega_1^2)(1 + \omega_2^2)} + 2\nu \text{Re} \left\{ \left(2\pi g^2 \hat{\Gamma}(\omega_1, \omega_2) + \frac{1}{2\pi} \right) \frac{1}{(1 + i\omega_1)(1 + i\omega_2)} \right\} \hat{C}_x(\omega_1) \hat{C}_x(\omega_2). \quad (55)$$

Using Eq. 49 to evaluate the term involving $\hat{\Gamma}(\omega_1, \omega_2)$ along with the expression we have already determined for $\psi_\phi(\tau, \tau')$, we obtain the solution

$$\psi_x(\tau, \tau') = \left[1 + \frac{\nu^2}{(1 + \omega_1^2)(1 + \omega_2^2) - \nu^2} \right] \left[1 + 2\nu \text{Re} \left\{ \frac{1}{(1 + i\omega_1)(1 + i\omega_2) - \nu} \right\} \left(2 - \frac{\nu^2}{(1 + \omega_1^2)(1 + \omega_2^2)} \right) \right] \hat{C}_x(\omega_1) \hat{C}_x(\omega_2), \quad (56)$$

which recovers Eq. 6 of the main text for $a = x$.

In computing the formulae for $\hat{\psi}_\phi(\omega_1, \omega_2)$ and $\hat{\psi}_x(\omega_1, \omega_2)$, one can use

$$\text{Re} \left\{ \frac{1}{(1 + i\omega_1)(1 + i\omega_2) - \nu} \right\} = \frac{1 - \nu - \omega_1 \omega_2}{(1 - \nu - \omega_1 \omega_2)^2 + (\omega_1 + \omega_2)^2}. \quad (57)$$